

Linear and nonlinear spectroscopy from quantum master equations

Jonathan H. Fetherolf¹ and Timothy C. Berkelbach^{1, a)}

Department of Chemistry and James Franck Institute, University of Chicago, Chicago, Illinois 60637 USA

We investigate the accuracy of the second-order time-convolutionless (TCL2) quantum master equation for the calculation of linear and nonlinear spectroscopies of multichromophore systems. We show that, even for systems with non-adiabatic coupling, the TCL2 master equation predicts linear absorption spectra that are accurate over an extremely broad range of parameters and well beyond what would be expected based on the perturbative nature of the approach; non-equilibrium population dynamics calculated with TCL2 for identical parameters are significantly less accurate. For third-order (two-dimensional) spectroscopy, the importance of population dynamics and the violation of the so-called quantum regression theorem degrade the accuracy of TCL2 dynamics. To correct these failures, we combine the TCL2 approach with a classical ensemble sampling of slow microscopic bath degrees of freedom, leading to an efficient hybrid quantum-classical scheme that displays excellent accuracy over a wide range of parameters. In the spectroscopic setting, the success of such a hybrid scheme can be understood through its separate treatment of homogeneous and inhomogeneous broadening. Importantly, the presented approach has the computational scaling of TCL2, with the modest addition of an embarrassingly parallel prefactor associated with ensemble sampling. The presented approach can be understood as a generalized inhomogeneous cumulant expansion technique, capable of treating multilevel systems with non-adiabatic dynamics.

I. INTRODUCTION

Non-adiabatic energy transfer in molecular systems represents a problem of broad interest in chemistry, physics, and materials science. In the condensed phase, these processes commonly occur with many comparable energy scales, precluding simple perturbative treatments of the dynamics such as Golden-rule-type rate theories. This class of problems has motivated the important development of accurate numerical techniques capable of evolving the electronic reduced density matrix and offering insight into the population dynamics of multi-level dissipative quantum systems.^{1–7} However, with few exceptions, elements of the reduced density matrix are basis-dependent and not directly observable. Instead, the principal experimental probes of energy transfer dynamics are ultrafast time-resolved spectroscopies, such as pump-probe transient absorption and coherent two-dimensional spectroscopy.^{8–13} In this manuscript, we evaluate the accuracy of perturbative, but non-Markovian, quantum master equations for the calculation of linear and nonlinear spectroscopies. In particular, we focus on systems characteristic of protein-protected biological chromophores. This class of problems has been the topic of intense study in the quantum dynamics community,^{14–21} in part because the environmental fluctuations exhibit long correlation times that challenge conventional theories.^{22,23}

The Hamiltonian for multichromophore systems can be generically written as the sum of an electronic (system) Hamiltonian, a nuclear (bath) Hamiltonian, and the interaction between the two, $H = H_s + H_b + V$. In the present manuscript, we consider a Frenkel exciton model of coupled chromophores, with the system Hamiltonian

$$H_s = \sum_m (\bar{\epsilon} + \epsilon_m) B_m^\dagger B_m + \sum_{mn} J_{mn} B_m^\dagger B_n, \quad (1)$$

where $\bar{\epsilon}$ is a mean excitation energy for the excited-state manifold (equal to 10,000–30,000 cm⁻¹ for visible-light absorbing chromophores), ϵ_m is the deviation from this mean excitation energy for site m , and J_{mn} is the electronic coupling between sites m and n . The operators B_m^\dagger and B_m create and annihilate localized excitations on site m and satisfy the commutation relation $[B_m, B_n^\dagger] = \delta_{mn}(1 - 2B_m^\dagger B_m)$. The bath Hamiltonian is that of the nuclear degrees of freedom in the electronic ground-state. The system-bath interaction can be generically decomposed into the form $V = \sum_a E_a F_a$ where E_a are bath operators and F_a are system operators. For simplicity, we consider the case

$$V = \sum_m E_m B_m^\dagger B_m, \quad (2)$$

where E_m is a collective bath operator whose fluctuations act to modulate the energy gap of molecular site m . An otherwise generic second-order perturbation theory in the system-bath interaction requires only the equilibrium time correlation function of the nuclear degrees of freedom in the electronic ground state,

$$C_m(t) = \text{Tr}_b \left\{ E_m(t) E_m(0) \rho_b^{\text{eq}} \right\} \quad (3)$$

where $E_m(t) = \exp(iH_b t/\hbar) E_m \exp(-iH_b t/\hbar)$. For simplicity, we assume nuclear degrees of freedom belonging to different molecular sites are uncorrelated. This approach is commonly pursued to account for dephasing dynamics via atomistic simulations; in this approach, classical molecular dynamics are used to generate trajectories for the evaluation of the energy gap autocorrelation function in Eq. (3), leading to the second-order cumulant approximation to the lineshape,^{8,24}

$$I_m(\omega) \propto \int_0^\infty dt e^{i\omega t} \exp \left[- \int_0^t dt_1 \int_0^{t_1} dt_2 C_m(t_2) \right]. \quad (4)$$

Strictly, the correlation function in Eq. (3) is a quantum time correlation function and a variety of approximate schemes exist to reconstruct a quantum time correlation function from its

^{a)}Electronic mail: berkelbach@uchicago.edu

classical counterpart.^{25,26} We note that the above formalism neglects energy transfer (or non-adiabatic effects) associated with the intermolecular couplings J_{mn} . In this $J_{mn} = 0$ limit of “pure dephasing,” the second order cumulant approximation is quantum mechanically exact if the E_m operators are linear in the coordinates of a harmonic bath;^{27,28} this linear coupling model will be adopted below. In the more general case of energy transfer associated with population relaxation, spectroscopy calculations require a more general approach to quantum dynamics, which we discuss in the next section.

II. SPECTROSCOPY, CORRELATION FUNCTIONS, AND THE QUANTUM REGRESSION THEOREM

In order to calculate spectroscopic observables, we augment our Hamiltonian with a light-matter interaction term to be treated via time-dependent perturbation theory,⁸

$$H_{\text{spec}}(t) = H - \boldsymbol{\mu} \cdot \mathbf{E}(t); \quad (5)$$

here, $\mathbf{E}(t)$ is a classical electric field and $\boldsymbol{\mu}$ is the dipole operator

$$\boldsymbol{\mu} = \sum_m \mu_m (B_m^\dagger + B_m) \quad (6)$$

where, via the Condon approximation, the dipole matrix element μ_m is independent of the bath degrees of freedom. For simplicity, here and henceforth we neglect the vectorial nature of the transition dipole matrix element.

Linear absorption spectra are calculated from the equilibrium time-correlation response function,

$$S^{(1)}(t) = \frac{i}{\hbar} \theta(t) \text{Tr} \{ [\boldsymbol{\mu}(t), \boldsymbol{\mu}] \rho^{\text{eq}} \} = \frac{i}{\hbar} \theta(t) \text{Tr} \{ \boldsymbol{\mu} \mathcal{G}(t) \boldsymbol{\mu}^\times \rho^{\text{eq}} \} \quad (7)$$

where $\boldsymbol{\mu}^\times A \equiv [\boldsymbol{\mu}, A]$ and the Liouville-space propagator is defined by $\mathcal{G}(t)A = e^{-iHt/\hbar} A e^{iHt/\hbar}$. Two-dimensional spectra are calculated from the third-order response function,

$$S^{(3)}(t_3, t_2, t_1) = \left(\frac{i}{\hbar} \right)^3 \theta(t_3) \theta(t_2) \theta(t_1) \times \text{Tr} \{ \boldsymbol{\mu} \mathcal{G}(t_3) \boldsymbol{\mu}^\times \mathcal{G}(t_2) \boldsymbol{\mu}^\times \mathcal{G}(t_1) \boldsymbol{\mu}^\times \rho^{\text{eq}} \}. \quad (8)$$

With exact quantum dynamics, the above expressions produce exact spectra that contain the effects of coherence dephasing as well as population relaxation, with explicit treatment of system-bath correlations spanning multiple light-matter interactions.

As a one-time observable, the linear-response function can be calculated exactly from the time evolution of a reduced density-like operator

$$\rho_\mu(t) \equiv \text{Tr}_b \{ \boldsymbol{\mathcal{G}}(t) \boldsymbol{\mu}^\times \rho^{\text{eq}} \} = \mathcal{G}_{\text{red}}(t, 0) \rho_\mu(0), \quad (9)$$

$$S^{(1)}(t) = \frac{i}{\hbar} \text{Tr}_s \{ \boldsymbol{\mu} \rho_\mu(t) \} = \frac{i}{\hbar} \text{Tr}_s \{ \boldsymbol{\mu} \mathcal{G}_{\text{red}}(t, 0) \rho_\mu(0) \}. \quad (10)$$

Therefore, any theory of reduced dynamics may be used to calculate the linear response function, such as a formally exact

time-convolutionless quantum master equation,^{29–33}

$$\frac{d\rho(t)}{dt} = -\frac{i}{\hbar} [H_s, \rho(t)] - \mathcal{R}(t) \rho(t) \equiv -\frac{i}{\hbar} \mathcal{L}_{\text{red}}(t) \rho(t), \quad (11)$$

$$\rho(t) = T \exp \left[-\frac{i}{\hbar} \int_0^t d\tau \mathcal{L}_{\text{red}}(\tau) \right] \rho(0) \equiv \mathcal{G}_{\text{red}}(t, 0) \rho(0), \quad (12)$$

where T is the time-ordering operator. Naturally, the lowest-order approximation to the time-dependent relaxation operator $\mathcal{R}(t)$ may be used; this is the second-order time convolutionless (TCL2) quantum master equation.³¹ Unlike the second cumulant approach described in Sec. I, the TCL2 master equation (detailed below) provides a perturbative description of population relaxation and coherence dephasing on equal footing. Importantly, in the absence of population relaxation, the TCL2 approximation yields uncoupled dephasing dynamics of the (in this case off-diagonal) reduced operator $\sigma(t)$ that are identical to those of the second-order cumulant approximation, and thus exact for linear coupling to a harmonic bath. In other words, the dynamical resummation inherent in the TCL2 approximation is exact for this example of the pure-dephasing problem (due to underlying Gaussian statistics). We emphasize that this exactness is independent of the number of bath degrees of freedom, the energy scales of the bath, or the strength of the system-bath coupling.

However, in the presence of population relaxation with $J_{mn} \neq 0$, the TCL2 approximation is no longer exact, and its range of validity is commonly understood to be restricted to the nearly-Markovian, weak-coupling limit under which it is typically derived. We will demonstrate that such statements are completely dependent on the observable and *not* determined exclusively by the energy scales in the Hamiltonian. In particular, we will show that for the same Hamiltonian, TCL2 predicts qualitatively incorrect non-equilibrium population dynamics but quantitatively accurate linear absorption lineshapes.

Unfortunately, the simplicity of the linear response function is not maintained for higher-order correlation functions. If we were to generalize Eqs. (9) and (10) to the third-order response function, we might be led to the tempting approximation

$$\begin{aligned} \tilde{S}^{(3)}(t_3, t_2, t_1) &= \left(\frac{i}{\hbar} \right)^3 \theta(t_3) \theta(t_2) \theta(t_1) \\ &\times \text{Tr}_s \{ \boldsymbol{\mu} \mathcal{G}_{\text{red}}(t_1 + t_2 + t_3, t_1 + t_2) \\ &\times \boldsymbol{\mu}^\times \mathcal{G}_{\text{red}}(t_1 + t_2, t_1) \boldsymbol{\mu}^\times \mathcal{G}_{\text{red}}(t_1, 0) \rho_\mu(0) \}, \end{aligned} \quad (13)$$

which can be shown to be consistent with a quantum version of Onsager’s regression hypothesis known as the quantum regression theorem (QRT).^{34,35} In general, the QRT is not exact.^{36,37} The exact multi-time correlation function is related to the approximate one by a number of correction terms, which are non-vanishing even to lowest-order in the system-bath interaction.^{38–40} To summarize, in the context of the current manuscript, *the rigorous calculation of nonlinear response functions requires more information than contained in quantum master equations.*

The violation of the QRT is intimately linked to the degree of non-Markovianity present in the reduced dynamics. For purely Markovian reduced dynamics, the QRT is exact.^{37,41} For weak system-bath coupling leading to nearly Markovian reduced dynamics, the corrections to the QRT are small. In this manuscript, we will study the accuracy of TCL2 dynamics, within the approximation implied by the QRT, Eq. (13), for the simulation of two-dimensional spectroscopy. Unsurprisingly, we find that the results deteriorate with increasing non-Markovianity due to stronger coupling or slower bath degrees of freedom.

In order to maintain the simplicity of quantum master equations while seeking broad applicability to nonlinear spectroscopy, we will evaluate the use of the “frozen modes” approach, recently introduced by one of us and co-workers.⁴² The method will be described in more detail below, but the idea is to simulate generically non-Markovian dynamics by an average over many independent nearly-Markovian trajectories. In each trajectory, the low-frequency bath degrees of freedom are dynamically arrested: they are removed from the master equation’s relaxation operator and treated as a source of static disorder. This frozen-mode approximation is obviously best for low-frequency (slow) degrees of freedom, which are precisely those that contribute to non-Markovian behavior and the inaccuracy of perturbative quantum master equations. Compared to the original problem, each individual trajectory in the frozen modes approach exhibits less non-Markovian behavior and weaker system-bath coupling. Because these are the same effects responsible for the violation of the QRT in nonlinear response calculations, we will demonstrate that the frozen-mode variant of TCL2 dynamics leads to accurate two-dimensional spectra, even in highly non-Markovian regimes.

III. MODEL AND METHODS

For the remainder of this work, we will adopt the common system-bath model that assumes a harmonic nuclear bath linearly coupled to the system’s excitation number operator, i.e. Eqs. (1) and (2) with

$$H_b = \frac{1}{2} \sum_m \sum_k (P_{m,k}^2 + \omega_{m,k}^2 Q_{m,k}^2), \quad (14)$$

$$E_m = \sum_k c_{m,k} Q_{m,k}, \quad (15)$$

where $P_{m,k}$ and $Q_{m,k}$ are the mass-weighted momentum and position of mode k belonging to the nuclear degrees of freedom of site m . For such a simplified form of the system-bath interaction, *all* properties are determined solely by the equilibrium autocorrelation function in Eq. (3),

$$\begin{aligned} C_m(t) &= \sum_k c_{m,k}^2 \text{Tr}_b \{ Q_{m,k}(t) Q_{m,k}(0) e^{-\beta H_b} \} / \text{Tr}_b e^{-\beta H_b} \\ &= \frac{\hbar}{\pi} \int_0^\infty d\omega J_m(\omega) \{ \coth(\beta \hbar \omega / 2) \cos(\omega t) - i \sin(\omega t) \}, \end{aligned} \quad (16)$$

where we have introduced the spectral density

$$J_m(\omega) = \frac{\pi}{2} \sum_k \frac{c_{m,k}^2}{\omega_{m,k}} \delta(\omega - \omega_{m,k}). \quad (17)$$

Note that the spectral density can be obtained from the real-part of the cosine-transform of the bath correlation function

$$J_m(\omega) = \tanh(\beta \hbar \omega / 2) \int_0^\infty dt \cos(\omega t) \text{Re} C_m(t), \quad (18)$$

which provides a way to extract a model spectral density from atomistic simulations of the energy gap autocorrelation function, as done recently for light-harvesting complexes.^{43,44} In the following, we assume all sites have identical spectral densities $J_m(\omega) = J(\omega)$ and employ an Ohmic spectral density with a high-frequency Lorentzian cutoff

$$J(\omega) = \frac{2\lambda\omega_c\omega}{\omega_c^2 + \omega^2}, \quad (19)$$

which follows from the assumption of an exponentially-decaying autocorrelation function (in the high-temperature limit), $\text{Re} C(t) = 2\lambda k_B T \exp(-\omega_c t)$. Therefore, the bath relaxation time is given by $\tau_c = 1/\omega_c$ and the magnitude of fluctuations is related to the reorganization energy $\lambda = (\hbar\pi)^{-1} \int_0^\infty d\omega J(\omega)/\omega$. We emphasize that most of our conclusions are not restricted to any particular form of $J(\omega)$, including those with arbitrary structure (as may be obtained from simulation). Specifically, we expect that the *accuracy* of our results is only weakly dependent on the form of the spectral density, and can be safely applied to any system-bath Hamiltonian exhibiting only linear coupling to a harmonic bath. However, while the method is entirely *applicable* to more general system-bath Hamiltonians, the accuracy is harder to assess. For example, we note that even for the pure-dephasing problem, the second cumulant is no longer exact for systems that are quadratically-coupled to harmonic baths.^{27,28}

A. Quantum master equations and TCL2

Introduced above, the TCL2 quantum master equation evolves reduced-density-like system operators $\sigma(t)$ according to the time-local equation of motion in Eq. (20). This equation of motion assumes a factorized initial condition of the total density-like operator $\rho(0) = \sigma(0)\rho_b(0)$, and we henceforth assume that the initial bath density operator is at equilibrium, $\rho_b(0) = \rho_b^{\text{eq}}$. We note that for Hamiltonians with a minimum excited-state gap that is much larger than thermal energy, the total equilibrium density operator is factorized to an excellent approximation, $\rho^{\text{eq}} \approx |0\rangle\langle 0| \rho_b^{\text{eq}}$, justifying factorized initial conditions for equilibrium correlation functions. In the basis of eigenstates of the system Hamiltonian, the TCL2 relaxation superoperator \mathcal{R} is a tensor with elements

$$\begin{aligned} \mathcal{R}_{\alpha\beta\gamma\delta}(t) &= \text{Tr}_s \{ |\alpha\rangle\langle\beta| \mathcal{R}(t) [|\delta\rangle\langle\gamma|] \} \\ &= \Gamma_{\delta\beta\alpha\gamma}^+(t) + \Gamma_{\delta\beta\alpha\gamma}^-(t) \\ &\quad - \delta_{\beta\delta} \sum_\zeta \Gamma_{\alpha\zeta\zeta\gamma}^+(t) - \delta_{\alpha\gamma} \sum_\zeta \Gamma_{\delta\zeta\zeta\beta}^-(t), \end{aligned} \quad (20)$$

with

$$\Gamma_{\alpha\beta\gamma\delta}^{\pm}(t) = \frac{1}{\hbar^2} \sum_m N_m^{\alpha\beta} N_m^{\gamma\delta} \Theta_m^{\pm}(\omega_{\gamma\delta}; t) \quad (21)$$

and

$$\Theta_m^{\pm}(\omega; t) = \int_0^t d\tau e^{-i\omega\tau} C_m(\pm\tau). \quad (22)$$

In the above, $N_m^{\alpha\beta} = \langle \alpha | B_m^{\dagger} B_m | \beta \rangle$ and $C_m(t)$ is given in Eq. (16). The relevant dimensionless parameter that controls the accuracy of weak-coupling master equations is roughly given by $\lambda k_B T / (\hbar \omega_c)^2$; in particular, very slow bath relaxation dynamics are a challenge as they violate the quasi-Markovian approximations inherent in such master equations. As such, we will also consider a quantum-classical hybrid scheme that microscopically treats slow nuclear degrees of freedom as static variables sampled from their respective canonical distributions, discussed next.

B. TCL2 master equation with frozen modes

The spectral density defined in Eq. (17) can formally be separated into fast and slow components under the condition that $J(\omega) = J_{\text{fast}}(\omega) + J_{\text{slow}}(\omega)$. In the ideal partitioning, the slow part is comprised of quasi-adiabatic modes that evolve much more slowly than the system and can safely be treated classically, while the fast part contains modes which evolve much more quickly than the system and therefore can be treated with nearly-Markovian weak-coupling theories.^{5,45,46} The partitioning between slow and fast parts of $J(\omega)$ can be done with a switching function,

$$J_{\text{slow}}(\omega) = s(\omega; \omega^*) J(\omega) \quad (23a)$$

$$J_{\text{fast}}(\omega) = [1 - s(\omega; \omega^*)] J(\omega), \quad (23b)$$

where $s(\omega; \omega^*)$ is a function which goes from a value of 1 at $\omega = 0$ to a value of 0 at a specified splitting frequency $\omega = \omega^*$. Following previous work^{42,45,46} we use the smooth switching function

$$s(\omega, \omega^*) = \begin{cases} [1 - (\omega/\omega^*)^2]^2 & : \quad \omega < \omega^* \\ 0 & : \quad \omega \geq \omega^*, \end{cases} \quad (24)$$

which avoids long-time oscillatory features in the bath correlation function. The free parameter ω^* determines the set of modes to be treated classically. Two example partitionings of an Ohmic-Lorentz spectral density are shown in Fig. 1.

While the slow modes could be treated with several different semiclassical techniques, including mean-field Ehrenfest dynamics,^{5,45,46} here we make the simplest approximation and treat the modes described by $J_{\text{slow}}(\omega)$ as completely frozen. In this case, positions of the slow degrees of freedom $Q_{m,k}$ are sampled from the Boltzmann distribution of a harmonic oscillator and used to alter the energy levels of the system Hamiltonian,

$$\epsilon_m \rightarrow \epsilon_m + \sum_{k \in \text{slow}} \bar{c}_{m,k} Q_{m,k}(0), \quad (25)$$

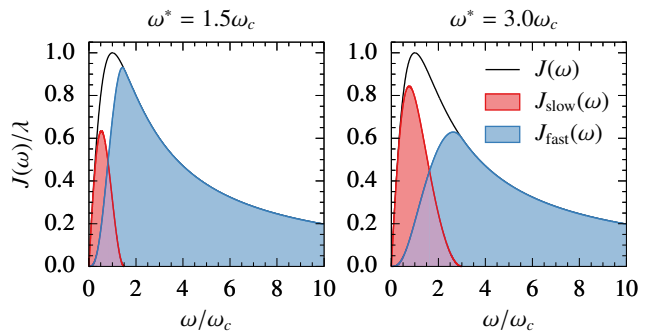


FIG. 1. Two example partitionings of an Ohmic-Lorentz spectral density using different values of the splitting frequency ω^* ; see Eqs. (23). Larger values of ω^* result in more modes being treated classically and fewer modes treated quantum mechanically, but perturbatively.

where $\bar{c}_{m,k}$ is a renormalized coupling constant due to the partitioning enforced by the switching function $S(\omega; \omega^*)$. This new system Hamiltonian is used with the *fast* part of the spectral density to perform a single realization of TCL2 dynamics. This process is repeated and averaged. Further details and discussion of the method can be found in Ref. 42.

In the spectroscopic context, the frozen modes are most physically interpreted as a source of inhomogeneous broadening. If the nuclear degrees of freedom are extremely slow, so as to appear effectively frozen during the decay of the dipole autocorrelation function, then this is the correct result. We emphasize that this inhomogeneous broadening is entirely microscopic because it originates from degrees of freedom in the total Hamiltonian; it is not an artificial, unidentified source of inhomogeneous broadening. When applied to linear absorption spectra of systems without non-adiabatic effects, this approach is equivalent to the inhomogeneous cumulant expansion described in Refs. 8 and 47, but differs for higher-order spectroscopies.

The combination of TCL2 dynamics with frozen-mode sampling (TCL2-FM) leads to many trajectories that are each *more Markovian* than the original problem. This property mitigates corrections to the QRT, which are not considered explicitly in this work. Furthermore, the TCL2-FM approach prevents the application of perturbation theory beyond its regime of validity (through the use of a faster, more weakly-coupled bath in the quantum master equation). As we show below, these two effects collectively produce semiquantitative accuracy in the prediction of nonlinear spectroscopy.

IV. RESULTS

A. Model parameters and methodological details

For simplicity, we present results for a system of two chromophores that has four accessible electronic states: the ground state, two states where each chromophore is separately excited, and one state where both chromophores are simul-

taneously excited. The absence of a quartic exciton-exciton interaction in Eq. (1) implies that the energy of the doubly-excited state is simply the sum of the excitation energies of the individual chromophores. In all results, we use the electronic parameters $\epsilon_1 = 50 \text{ cm}^{-1}$, $\epsilon_2 = -50 \text{ cm}^{-1}$ and $J_{12} = 100 \text{ cm}^{-1}$, along with the bath parameters $\omega_c^{-1} = 300 \text{ fs}$ and $T = 300 \text{ K}$. The reorganization energy λ will be varied. The bath frequency and temperature lead to energy scales $\hbar\omega_c = 18 \text{ cm}^{-1}$ and $k_B T = 208 \text{ cm}^{-1}$, i.e. all energy scales are comparable, with the bath frequency being the smallest.

Our TCL2 dynamics are generated with a fourth-order Runge-Kutta integrator. For TCL-FM calculations, the total spectral density was discretized into 300 modes, and those with $\omega > \omega^*$ were discarded. We performed 2×10^4 realizations of frozen-mode sampling to converge the dynamical observables. For all frozen-mode calculations, we use a splitting frequency that characterizes the timescale of isolated electronic dynamics, $\omega^* = [(\epsilon_1 - \epsilon_2)^2 + 4J_{12}^2]^{1/2}/6\hbar$. Other choices that differ by factors of order one give similar qualitative results, and occasionally better quantitative results, but we find that the above form is reasonable over a broad range of parameters and observables.

All approximate results will be compared to numerically exact results obtained with the hierarchical equations of motion (HEOM),^{1,48,49} for the bath parameters used in our results, the HEOM calculations required zero Matsubara frequencies (i.e. the high-temperature approximation with $K = 0$), but as many as $L = 20$ levels in the hierarchy. For spectroscopy calculations, we use transition dipole matrix elements satisfying $\mu_1/\mu_2 = -5$ and spectra will be presented with arbitrary units. All calculations were performed with our open-source quantum dynamics package pyrho.⁵⁰

B. Linear spectroscopy and population dynamics

In the frequency domain, we present the imaginary (absorptive) part of the linear-response susceptibility,

$$\chi''(\omega) = \text{Im} \int_0^\infty dt e^{i\omega t} S^{(1)}(t). \quad (26)$$

Again we emphasize that for the model Hamiltonian adopted here, the TCL2 master equation is identical to the second-cumulant approximation and exactly solves the pure-dephasing lineshape problem. In the case of excited-state electronic coupling $J \neq 0$, the TCL2 generalizes the second cumulant approximation. While it is not exact, the results are remarkably accurate, as shown in the right-hand column of Fig. 2, even for significant coupling to a slow bath. The TCL2-FM approach yields very minor quantitative improvements, which confirms that those local-frequency modes treated as frozen are properly interpreted as giving rise to inhomogeneous broadening.

Unlike the non-Markovian TCL2-based approaches, the Markovian Redfield theory predicts incorrect spectra, with an accuracy that deteriorates for increasing reorganization energy or increasing bath relaxation times. This can be

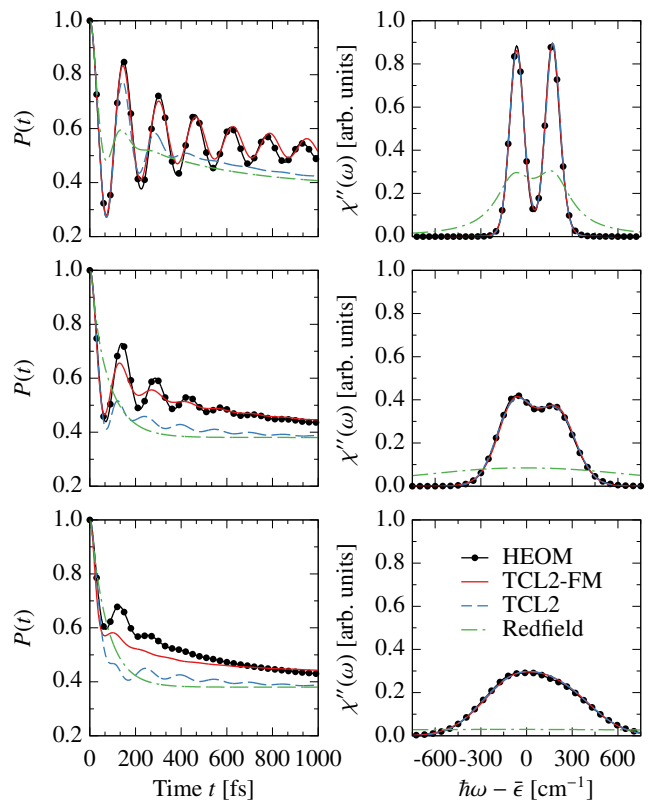


FIG. 2. Population dynamics of the photo-excited higher-energy chromophore (left column) and linear absorption spectra (right column) with $\lambda = 10 \text{ cm}^{-1}$, 50 cm^{-1} , and 150 cm^{-1} (top to bottom).

understood simply from the Markovian limit of the relevant pure-dephasing term in the TCL2 tensor: $1/T_2^* = \hbar^{-1} [J(\omega)n(\omega)]_{\omega=0}$ where $n(\omega)$ is the Bose-Einstein distribution function. For the Ohmic-Lorentz spectral density employed here, one finds $1/T_2^* = 2\lambda k_B T / \hbar\omega_c^2$. As shown in Fig. 2, this Markovian theory predicts linewidths that are much too large.

This large discrepancy between two weak-coupling theories (Markovian Redfield theory and non-Markovian TCL2-based theories) is quite surprising given the perturbative nature of both approaches. In the left-hand column panels of Fig. 2, we show the population relaxation dynamics generated by the same methods, using the initial condition $\rho(0) = |1\rangle\langle 1| \rho_b^{\text{eq}}$. Clearly, Redfield theory and conventional TCL2 fail in a similar manner as the perturbation becomes large. The TCL2-FM approach now yields results that are quite different than vanilla TCL2, and the former predicts population dynamics that are in good agreement with the numerically exact HEOM results. These observations demonstrate one of our main conclusions: the accuracy of a given dynamical technique depends on the observable. More specifically, TCL2-based approaches are well-suited to the evolution of electronic coherences; we believe that this is because TCL2 reduces to the exact second-cumulant solution for pure-dephasing problems. Population dynamics are less accurate.

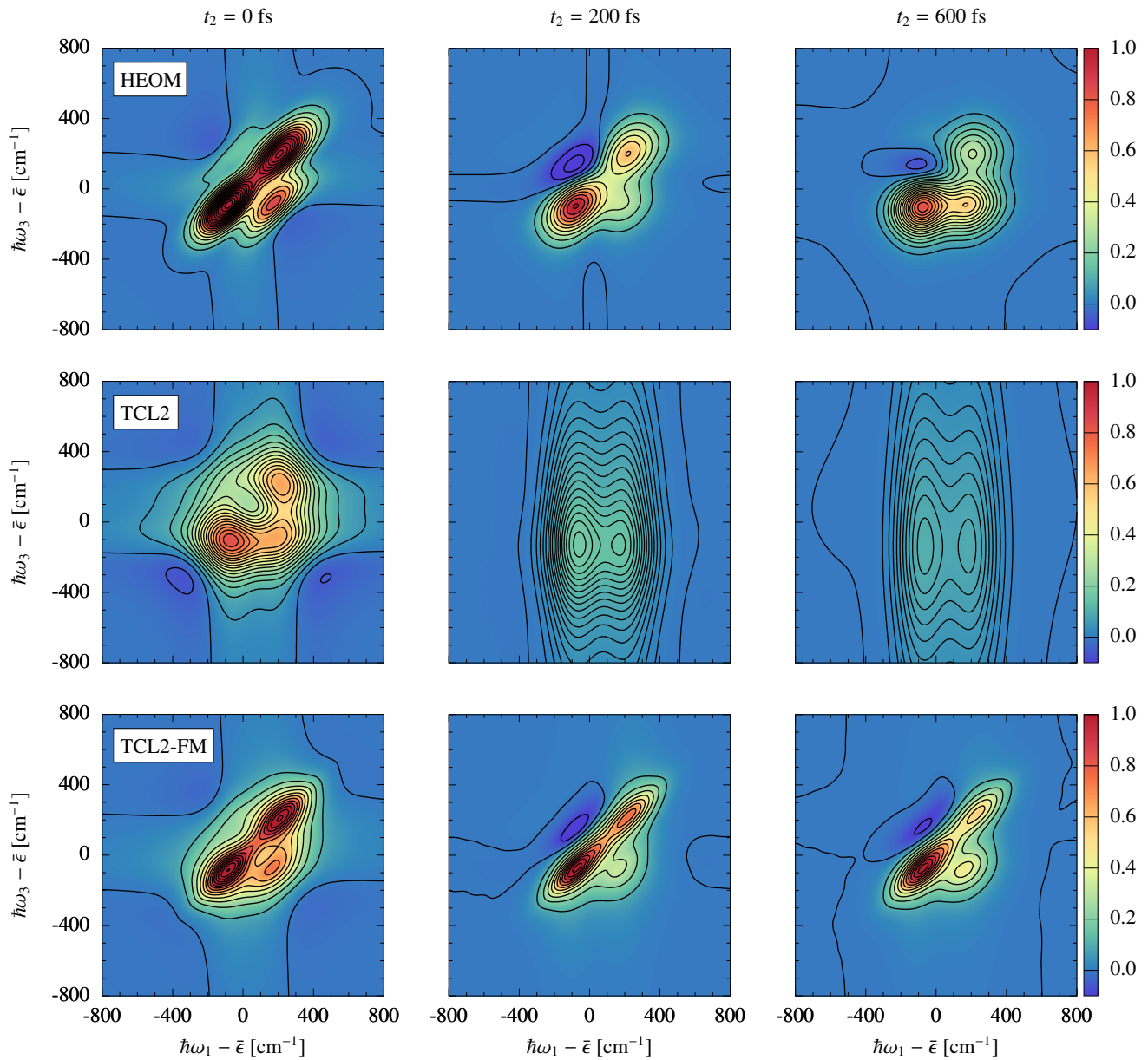


FIG. 3. Two-dimensional photon echo spectra for a model dimer with $\lambda = 50 \text{ cm}^{-1}$. Waiting times are shown and increase from left to right. Exact results (top row) are compared with the predictions of TCL2 (middle) and TCL2-FM (bottom row).

C. Third-order nonlinear spectroscopy

Compared to linear response considered above, third-order nonlinear spectroscopy is a more challenging test, due to the simultaneous importance of coherence and population dynamics. As discussed in Sec. II, nonlinear spectroscopy presents an additional complication for non-Markovian quantum master equations in the form of violations to the QRT.

We present two-dimensional electronic spectra, obtained by Fourier transforming over the pump (t_1) and probe (t_3) time delays, resolved by the population waiting time t_2 . In particular, we simulate the photon echo spectrum, generated by six terms in the rotating wave approximation associated with

rephasing (rp) and non-rephasing (nr) pathways,

$$A(\omega_3, t_2, \omega_1) = \text{Re} \int_0^\infty dt_1 \int_0^\infty dt_3 \left\{ e^{i(\omega_1 t_1 + \omega_3 t_3)} R_{\text{rp}}(t_3, t_2, t_1) + e^{i(-\omega_1 t_1 + \omega_3 t_3)} R_{\text{nr}}(t_3, t_2, t_1) \right\}. \quad (27)$$

In the above,

$$R_{\text{rp}}(t_3, t_2, t_1) = R_2(t_3, t_2, t_1) + R_3(t_3, t_2, t_1) + R_1^*(t_3, t_2, t_1), \quad (28a)$$

$$R_{\text{nr}}(t_3, t_2, t_1) = R_1(t_3, t_2, t_1) + R_4(t_3, t_2, t_1) + R_2^*(t_3, t_2, t_1), \quad (28b)$$

and

$$R_1(t_3, t_2, t_1) = \text{Tr}\{\mu(t_1 + t_2 + t_3)\mu(0)\rho^{\text{eq}}\mu(t_1)\mu(t_1 + t_2)\}, \quad (29\text{a})$$

$$R_2(t_3, t_2, t_1) = \text{Tr}\{\mu(t_1 + t_2 + t_3)\mu(0)\rho^{\text{eq}}\mu(t_1)\mu(t_1 + t_2)\}, \quad (29\text{b})$$

$$R_3(t_3, t_2, t_1) = \text{Tr}\{\mu(t_1 + t_2 + t_3)\mu(t_1 + t_2)\rho^{\text{eq}}\mu(0)\mu(t_1)\}, \quad (29\text{c})$$

$$R_4(t_3, t_2, t_1) = \text{Tr}\{\mu(t_1 + t_2 + t_3)\mu(t_1 + t_2)\mu(t_1)\mu(0)\rho^{\text{eq}}\}. \quad (29\text{d})$$

For a moderate reorganization energy of $\lambda = 50 \text{ cm}^{-1}$, our results are shown in Fig. 3 for three values of the waiting time t_2 . Although TCL2 dynamics are qualitatively correct at $t_2 = 0$, this accuracy degrades with increasing waiting times. In particular, the spectra become artificially broadened along the ω_3 axis – as discussed in Ref. 51 – and completely fail to describe the four-peak structure and regions of negativity. In contrast, the TCL2-FM two-dimensional spectra are in qualitative agreement with the exact results, reproducing the appropriate peak shapes, spectral features, and timescales. The TCL2-FM results show an unphysical diagonal elongation at long waiting times due to the completely frozen modes that are unable to relax. We have found that using a smaller splitting frequency (i.e. freezing fewer modes) does improve the long-time results at the expense of short-time results. This observations suggests an interesting time-dependent frozen-modes scheme – where modes are successively unfrozen at times longer than their characteristic relaxation time – though we do not pursue this approach here. We conclude that the computationally efficient TCL2-FM approach yields accurate coherence and population dynamics, while mitigating correction terms due to violation of the QRT, leading to qualitatively correct two-dimensional spectra. Although we only show one parameter set for simplicity, we have tested other parameter sets and find that the TCL2-FM accuracy is robust over a wide range of Hamiltonians.

For a simpler representation of the third-order response, we also present the time-resolved pump-probe spectra, obtained by setting $t_1 = 0$ (or equivalently, integrating over ω_1). We note that the correlation functions contributing to pump-probe spectroscopy are two-point nonequilibrium correlation functions, which should depend sensitively on the accuracy of excited-state population dynamics and exhibit nontrivial corrections to the QRT.^{38,39} For the same parameters as in Fig. 3, we present the pump-probe spectra in Fig. 4. Consistent with our findings for the full two-dimensional spectra, we see that TCL2 dynamics are accurate at zero waiting time, but completely wrong for nonzero waiting times; the spectra are much too broad and lacking multi-peaked structure. TCL2-FM dynamics cures these deficiencies and predicts accurate pump-probe spectra.

V. CONCLUSIONS

We have investigated the accuracy of the second-order time-convolutionless (TCL2) quantum master equation for the prediction of linear and third-order time-resolved spectroscopy. We have argued that TCL2 dynamics generalizes

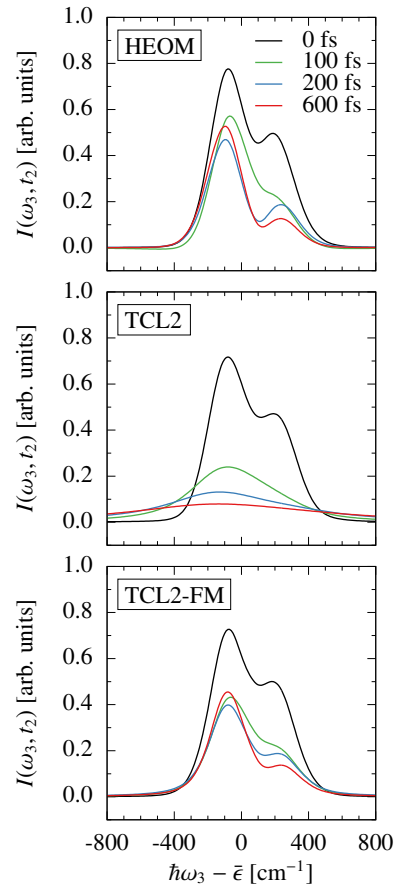


FIG. 4. Pump-probe spectra $I(\omega_3, t_2)$ obtained from two-dimensional photon echo data presented in Fig. 3, via integration over the ω_1 axis. Waiting times t_2 are given in the legend.

the second-cumulant approximation to problems exhibiting excited-state electronic coupling leading to non-adiabatic dynamics and population relaxation. For many contemporary problems concerning the dynamics of multichromophore systems, the bath timescales are too slow to permit classic Markovian theories of lineshapes. For such systems, the TCL2 approach generates nearly-exact linear-response spectra, even though simulations of population dynamics – using the same Hamiltonian parameters – are grossly in error.

In contrast, the TCL2 approximation breaks down away from its perturbative regime when used to simulate nonlinear spectroscopies. We have attributed this failure to two distinct effects: the greater importance of population dynamics and the violation of the quantum regression theorem (QRT). By partitioning microscopic bath degrees of freedom into fast and slow sets, and treating the latter as frozen variables sampled from a thermodynamic ensemble, we have argued that the TCL2-FM approach alleviates both of these problems. Physically, the TCL2-FM formalism treats modes responsible for highly non-Markovian dynamics as a source of inhomogeneous broadening; the resulting Hamiltonian exhibits dynamics which are consequently more Markovian and thus well-described by weak-coupling, TCL2-type quantum mas-

ter equations. It will be interesting to implement the second-order corrections to the QRT, in order to assess their relative importance in the prediction of nonlinear spectra. Work along these lines is currently in progress.

Importantly, unlike many reduced quantum dynamics techniques, the formalism of perturbative quantum master equations is not tied to specific forms of the bath Hamiltonian or the system-bath interaction, as long as multi-point equilibrium correlation functions of isolated bath operators can be computed. Nonetheless, the accuracy of such approaches remains to be assessed for more generic Hamiltonians, but the absence of numerically exact results makes this challenging.

Our findings have implications for other quantum dynamics techniques. In particular, we recall that the hierarchical equations of motion (HEOM) reduce to time-convolutionless and time-convolution quantum master equations when the hierarchy is truncated at low order.^{52,53} These low-order HEOM calculations will exhibit the same features described here. For linear spectroscopy, this observation argues strongly for the use of the time-convolutionless closure⁵² of the hierarchy, in support of the numerical observations made in Refs. 54 and 55. For nonlinear spectroscopy, low-order approximations will also violate the QRT, and higher levels in the hierarchy will be needed in order to eliminate these (neglected) corrections.

With regards to computational cost, the TCL2-FM approach is extremely attractive. In its conventional form, presented here, it scales only as MN_s^4 , where M is a parallel prefactor associated with frozen-mode ensemble sampling and N_s is size of the system Hilbert space; this scaling arises from the action of the relaxation tensor on the reduced density matrix. Because the frozen-modes approach leads to more Markovian dynamics, it is tempting to explore a stochastic unraveling of the reduced density matrix.^{31,35,56–58} This latter approach replaces a single reduced density matrix simulation by an average over *wavefunction* dynamics with stochastic relaxation events. This procedure would have a scaling of LMN_s^2 , where L is a parallel prefactor associated with the stochastic dynamics. We thus anticipate an accurate method which only requires many parallel simulations of system-wavefunction dynamics, each scaling like N_s^2 for generically non-sparse system Hamiltonians; it is hard to imagine a more attractive computational cost with comparable qualitative accuracy over an extremely broad range of Hamiltonian parameters.

ACKNOWLEDGMENTS

We thank Dr. Roel Tempelaar and Prof. Jim Skinner for helpful discussions. This research was supported by start-up funds from the University of Chicago. Calculations were performed with resources provided by the University of Chicago Research Computing Center (RCC) and we thank Dr. Jonathan Skone of the RCC for assistance.

¹Y. Tanimura and R. K. Kubo, *J. Phys. Soc. Jpn.* **58**, 101 (1989).

²C. H. Mak and D. Chandler, *Phys. Rev. A* **41**, 5709 (1990).

³D. E. Makarov and N. Makri, *Chem. Phys. Lett.* **221**, 482 (1994).

- ⁴M. Beck, A. Jackle, G. A. Worth, and H.-D. Meyer, *Phys. Rep.* **324**, 1 (2000).
- ⁵M. Thoss, H. Wang, and W. H. Miller, *J. Chem. Phys.* **115**, 2991 (2001).
- ⁶E. R. Dunkel, S. Bonella, and D. F. Coker, *J. Chem. Phys.* **129**, 114106 (2008).
- ⁷H.-T. Chen, G. Cohen, and D. R. Reichman, *J. Chem. Phys.* **146**, 054105 (2017).
- ⁸S. Mukamel, *Principles of Nonlinear Optical Spectroscopy* (Oxford University Press, 1995).
- ⁹J. D. Hybl, A. W. Albrecht, S. M. Gallagher Faeder, and D. M. Jonas, *Chem. Phys. Lett.* **297**, 307 (1998).
- ¹⁰S. Mukamel, *Annu. Rev. Phys. Chem.* **51**, 691 (2000).
- ¹¹D. M. Jonas, *Annu. Rev. Phys. Chem.* **54**, 425 (2003).
- ¹²T. Brixner, J. Stenger, H. M. Vaswani, M. Cho, R. E. Blankenship, and G. R. Fleming, *Nature* **434**, 625 (2005).
- ¹³G. S. Engel, T. R. Calhoun, E. L. Read, T.-K. Ahn, T. T. Mancal, Y.-C. Cheng, R. E. Blankenship, and G. R. Fleming, *Nature* **446**, 782 (2007).
- ¹⁴S. Jang, Y. C. Cheng, D. R. Reichman, and J. D. Eaves, *J. Chem. Phys.* **129**, 101104 (2008).
- ¹⁵M. B. Plenio and S. F. Huelga, *New J. Phys.* **10**, 113019 (2008).
- ¹⁶M. Mohseni, P. Rebentrost, S. Lloyd, and A. Aspuru-Guzik, *J. Chem. Phys.* **129**, 174106 (2008).
- ¹⁷P. Huo and D. F. Coker, *J. Chem. Phys.* **133**, 184108 (2010).
- ¹⁸J. Wu, F. Liu, Y. Shen, J. Cao, and R. J. Silbey, *New J. Phys.* **12**, 105012 (2010).
- ¹⁹A. Kolli, A. Nazir, and A. Olaya-Castro, *J. Chem. Phys.* **135**, 154112 (2011).
- ²⁰V. Tiwari, W. K. Peters, and D. M. Jonas, *Proc. Natl. Acad. Sci.* **110**, 1203 (2013).
- ²¹R. Tempelaar, T. L. C. Jansen, and J. Knoester, *J. Phys. Chem. B* **118**, 12865 (2014).
- ²²A. Ishizaki and G. R. Fleming, *J. Chem. Phys.* **130**, 234110 (2009).
- ²³A. Ishizaki and G. R. Fleming, *J. Chem. Phys.* **130**, 234111 (2009).
- ²⁴R. Kubo, *Adv. Chem. Phys.* **15**, 101 (1969).
- ²⁵S. A. Egorov, K. F. Everitt, and J. L. Skinner, *J. Phys. Chem. A* **103**, 9494 (1999).
- ²⁶S. A. Egorov, E. Rabani, and B. J. Berne, *J. Phys. Chem. B* **103**, 10978 (1999).
- ²⁷J. L. Skinner and D. Hsu, *J. Phys. Chem.* **90**, 4931 (1986).
- ²⁸D. Reichman, R. J. Silbey, and A. Suárez, *J. Chem. Phys.* **105**, 10500 (1996).
- ²⁹F. Shibata, Y. Takahashi, and N. Hashitsume, *J. Stat. Phys.* **17**, 171 (1977).
- ³⁰S. Chaturvedi and F. Shibata, *Z. Phys. B Condens. Matter* **35**, 297 (1979).
- ³¹H.-P. Breuer and F. Petruccione, *The Theory of Open Quantum Systems* (Oxford University Press, 2007).
- ³²B. Yoon, J. M. Deutch, and J. H. Freed, *J. Chem. Phys.* **62**, 4687 (1975).
- ³³S. Mukamel, I. Oppenheim, and J. Ross, *Phys. Rev. A* **17**, 1988 (1978).
- ³⁴M. Lax, *Phys. Rev.* **129**, 2342 (1963).
- ³⁵P. Gardiner and P. Zoller, *Quantum Noise* (Springer-Verlag, Berlin, 2004).
- ³⁶G. W. Ford and R. O'Connell, *Phys. Rev. Lett.* **77**, 798 (1996).
- ³⁷S. Swain, *J. Phys. A. Math. Gen.* **14**, 2577 (1999).
- ³⁸D. Alonso and I. de Vega, *Phys. Rev. Lett.* **94**, 1 (2005).
- ³⁹D. Alonso and I. de Vega, *Phys. Rev. A - At. Mol. Opt. Phys.* **75**, 052108 (2007).
- ⁴⁰H. S. Goan, P. W. Chen, and C. C. Jian, *J. Chem. Phys.* **134** (2011), 10.1063/1.3570581.
- ⁴¹N. Gisin, *J. Mod. Opt.* **40**, 2313 (1993).
- ⁴²A. Montoya-Castillo, T. C. Berkelbach, and D. R. Reichman, *J. Chem. Phys.* **143**, 194198 (2015).
- ⁴³S. Valleau, A. Eisfeld, and A. Aspuru-Guzik, *J. Chem. Phys.* **137**, 224103 (2012).
- ⁴⁴M. K. Lee and D. F. Coker, *J. Phys. Chem. Lett.* **7**, 3171 (2016).
- ⁴⁵T. C. Berkelbach, D. R. Reichman, and T. E. Markland, *J. Chem. Phys.* **136**, 034113 (2012).
- ⁴⁶T. C. Berkelbach, T. E. Markland, and D. R. Reichman, *J. Chem. Phys.* **136**, 084104 (2012).
- ⁴⁷L. E. Fried and S. Mukamel, *Adv. Chem. Phys.* **84**, 435 (1993).
- ⁴⁸A. Ishizaki and Y. Tanimura, *J. Phys. Soc. Japan* **74**, 3131 (2005).
- ⁴⁹R.-X. Xu and Y. Yan, *Phys. Rev. E* **75**, 031107 (2007).

- ⁵⁰“pyrho: a python package for reduced density matrix techniques,” <https://github.com/berkelbach-group/pyrho>.
- ⁵¹A. Ishizaki and Y. Tanimura, *Chem. Phys.* **347**, 185 (2008).
- ⁵²R. X. Xu, P. Cui, X. Q. Li, Y. Mo, and Y. Yan, *J. Chem. Phys.* **122**, 041103 (2005).
- ⁵³M. Xu, L. Song, K. Song, and Q. Shi, *J. Chem. Phys.* **146**, 064102 (2017).
- ⁵⁴L. Chen, R. Zheng, Q. Shi, and Y. Yan, *J. Chem. Phys.* **131**, 094502 (2009).
- ⁵⁵L. Chen, R. Zheng, Q. Shi, and Y. Yan, *J. Chem. Phys.* **132**, 024505 (2010).
- ⁵⁶P. Zoller, M. Marte, and D. Walls, *Phys. Rev. A* **35**, 198 (1987).
- ⁵⁷N. Gisin and I. C. Percival, *J. Phys. A: Math. Gen.* **25**, 5677 (1992).
- ⁵⁸H. J. Carmichael, *Phys. Rev. Lett.* **70**, 2273 (1993).